Chemical Vapor-Deposited Amorphous Silicon Nitride

Chemical Vapor-Deposited Amorphous Silicon Nitride*

Toshio HIRAI, Koichi NIIHARA, Shinsuke HAYASHI
and Takashi GOTO

The Research Institute for Iron, Steel and Other Metals

(Received December 16, 1976)

Synopsis

Chemical vapor-deposited amorphous Si_3N_4 (CVD-amorphous Si_3N_4) up to 4.2 mm in thickness has been prepared from a gaseous mixture of NH_3 and H_2-carried $SiCl_4$ under various deposition conditions. The formation of the CVD-amorphous Si_3N_4 depended strongly on the deposition temperature, total gas pressure and gas flow rate.

The CVD-amorphous Si_3N_4 prepared at 1100~1300°C does not crystallize by heating at each deposition temperature. Their density and deposition rate are markedly dependent on deposition conditions and have maximum values of 3.00 g/cm^3 (94% of the theoretical density of α-Si_3N_4) and 0.36 mm/hr, respectively.

The Vickers microhardness of the CVD-amorphous Si_3N_4 at room temperature varies between 2200 and 3200 kg/mm^2 according to its deposition conditions. The hardness at 1300°C is 1200~1300 kg/mm^2. The thermal conductivity was 0.010 cal/cm/sec/°C at 20°C and 0.012 cal/cm/sec/°C at 1300°C. The thermal expansion coefficient at 20~1200°C is 2.99 ± 0.05/°C.

The formation mechanism and the effect of gas flow patterns on the deposition rate of the CVD-amorphous Si_3N_4 are also discussed.

I. Introduction

Recently there has been steady interest in amorphous materials because of their superior chemical and physical properties.[1-4] The methods for the synthesis of amorphous materials are, in general, divided into two ways; rapid cooling from the liquid state and deposition from the gas phase. The chemical vapor deposition method (CVD) belongs to the latter.

It is well known that amorphous Si_3N_4 can be prepared by CVD.[5] Deposition of the CVD-amorphous Si_3N_4 has been carried out using various silicon compounds such as silane,[5-7] silicon tetrachloride,[6-9] silicon tetrafluoride,[10]

* The **1666th** report of the Research Institute for Iron, Steel and Other Metals.

(1) T. Masumoto and R. Maddin, Acta Met., **19** (1971), 191.
(2) H. Jones and C. Suryanarayana, J. Mater. Sci., **8** (1973), 705.
(3) M. Naka, K. Hashimoto and T. Masumoto, J. Japan Inst. Metals, **38** (1974), 835.
(4) T. Egami, P.J. Flanders and C.D. Graham, Jr., Appl. Phys. Lett., **26** (1975), 128.
(5) K.E. Bean, P.S. Glein, R.L. Yeakley and W.R. Runyan, J. Electrochem. Soc., **114** (1967), 733.
(6) T.L. Chu, C.H. Lee and G.A. Gruber, ibid, **114** (1967), 717.
(7) A.C. Airey, S. Clarke and P. Popper, Proc. Brit. Ceram. Soc., **22** (1973), 305.
(8) M.J. Grieco, F.L. Worthing and B. Schwartz, J. Electrochem. Soc., **115** (1968), **525**.
(9) B.E. Deal, E.L. Machenna and P.L. Castro, ibid, **116** (1969), 997.
(10) F. Galasso, U. Kuntz and W.J. Croft, J. Amer. Ceram. Soc., **55** (1972), 431.

silicon tetrabromide[11] and silica[12] as the source material. In general, the SiH_4-NH_3 and $SiCl_4$-NH_3 systems are widely employed. However, most of the preivous works on the CVD-amorphous Si_3N_4 have been concerned with the preparation of very thin films ($\sim 10^3$ Å) as insulators and diffusion masks for semiconductor devices.[5,6,8,9]

Bean et al.[5] reported that the Young's modulus and the breaking strength of the CVD-amorphous Si_3N_4 films of 8 μm thickness deposited from the SiH_4-NH_3 system were 6700 kg/mm^2 and 47 kg/mm^2, respectively. However, little work dealing with the CVD-amorphous Si_3N_4 has been reported.

In the present study, the massive CVD-amorphous Si_3N_4 up to 4.2 mm in thickness was prepared using the $SiCl_4$-NH_3-H_2 system. This paper describes a method for preparing the massive CVD-amorphous Si_3N_4, the effects of deposition temperature (T_{dep}), total gas pressure (P_{tot}) and gas flow rate (FR) on the structure, density and deposition rate of the amorphous deposits, and some of its properties.

II. Experimental procedure

II. 1 Preparation of CVD-amorphous Si_3N_4

Si_3N_4 was deposited on a graphite substrate using a gaseous mixture of NH_3 and H_2-carried $SiCl_4$. Although ammonolysis of $SiCl_4$ which forms Si_3N_4 involves a complicated reaction sequence, it would be thought to follow the reaction

$$3\,SiCl_4 + 4NH_3 \rightarrow Si_3N_4 + 12\,HCl \qquad (1)$$

The experimental arrangement and the reaction chamber are illustrated in Fig. 1. The process for preparing the CVD-amorphous Si_3N_4 has been fully described

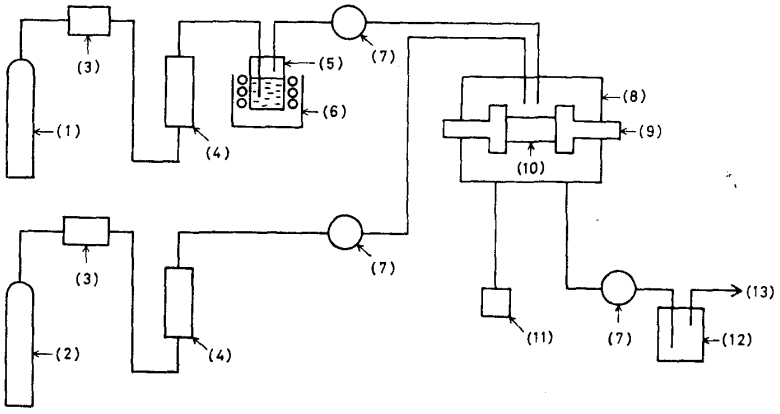

Fig. 1. Schematic diagram of the CVD-amorphous Si_3N_4 deposition apparatus.
(1) H_2 gas; (2) NH_3 gas; (3) gas purifier; (4) flowmeter; (5) $SiCl_4$ reservoir; (6) constant temperature bath; (7) pressure regulator; (8) reaction chamber; (9) electrode; (10) heater (substrate); (11) manometer; (12) cold trap; (13) rotary pump.

(11) L.A. Aboaf, J. Amer. Ceram. Soc., **116** (1969), 1736.
(12) K. Kijima, N. Setaka, M. Ishii and H. Tanaka, ibid, **56** (1973), 346.

Table 1. The preparation conditions of the CVD-amorphous Si_3N_4.

Heating method	Direct heating of graphite substrate
Deposition temperature (T_{dep}), °C	1100 to 1500
Total gas pressure (P_{tot}), Torr	5 to 100
Gas flow rate (FR), cm³/min	
$FR(H_2)$	400, 700, 1000
$FR(SiCl_4)$	100, 170, 260
$FR(NH_3)$	60, 60, 60

in a previous paper.[13] The conditions of preparation are summarized in Table 1. The flow rate ratio of $SiCl_4$ vapor to H_2 gas, $FR(SiCl_4)/FR(H_2)$, was fixed at about 0.26 in all deposition runs.

II. 2 Characterization of CVD-amorphous Si_3N_4

As-deposited surfaces of the CVD-amorphous Si_3N_4 were examined by optical and scanning electron microscopy.[13]

X-ray measurements were made for powdered samples with a diffractometric unit using Ni-filtered CuK_α radiation. The powdered samples were also examined by transmission electron microscopy and selected area diffractometry.

The silicon and oxygen contents in the CVD-amorphous Si_3N_4 were determined by electron probe microanalysis using high-purity silicon and fused silica as standard samples.

The density of the CVD-amorphous Si_3N_4 was determined by a displacement technique using toluene. The deposits were cut perpendicular to the substrate surface and then metallographically polished. The deposit thickness was measured at about 20 points of the specimen by a traveling microscope, and the values were averaged.

The deposition rate constant (k) is written as

$$(\Delta W)^n = kt\,, \tag{2}$$

where ΔW is the weight increase of the deposit per unit surface area of the substrate, n the order of reaction, and t the deposition time. Since ΔW is equal to the product of density (D) and thickness of deposit (x), we obtain

$$(Dx)^n = kt\,. \tag{3}$$

Here n can be determined from the time dependence of the thickness.

Vickers microhardness (VMH) measurements of the deposition surface and the cross-section were made using an AKASHI Vickers hardness tester (Model: MVK, type: D, apex angle: 136°) equipped with an optical microscope. Indentions were made under a load of 100 g for 30 sec. The Vickers microhardness at high temperatures up to 1300°C was also measured in vacuum or Ar atmosphere using a high temperature hardness tester (NIKON-QM).

Thermal diffusivity, specific heat and thermal conductivity were measured in

(13) K. Niihara and T. Hirai, J. Mater. Sci., **11** (1967), 593.

the temperature range of 20 to 1300°C using a laser-flash thermal constant analyzer (SHINKU RIKO, Model: TC-3000). The specimen used were in the form of a circular disk of 5 mm in diameter and 1 mm in thickness.

Thermal expansion was measured at a temperature between 20 and 1500°C using a RIGAKU thermomechanical analyzer (Model: TMA). Length of samples ranged from 10 to 15 mm. Aluminium oxide and fused silica were used as standard specimens.

III. Results

III. 1 Preparation conditions of CVD-amorphous Si_3N_4

Preparation of the CVD-amorphous Si_3N_4 depended markedly on T_{dep} and P_{tot}. As shown in Fig. 2 the amorphous deposits were obtained in the A region, whereas the crystalline deposits with the α-type structure were produced in the C region. The amorphous-crystalline boundary (A-C boundary) was affected by the flow rate of $SiCl_4$ vapor. At FR($SiCl_4$) = 100 ~ 170 cm³/min, the A-C boundary is indicated by a solid line in Fig. 2. The broad A-C boundary where the amorphous and crystalline deposits were heterogeneously obtained was observed at FR ($SiCl_4$) = 260 cm³/min.

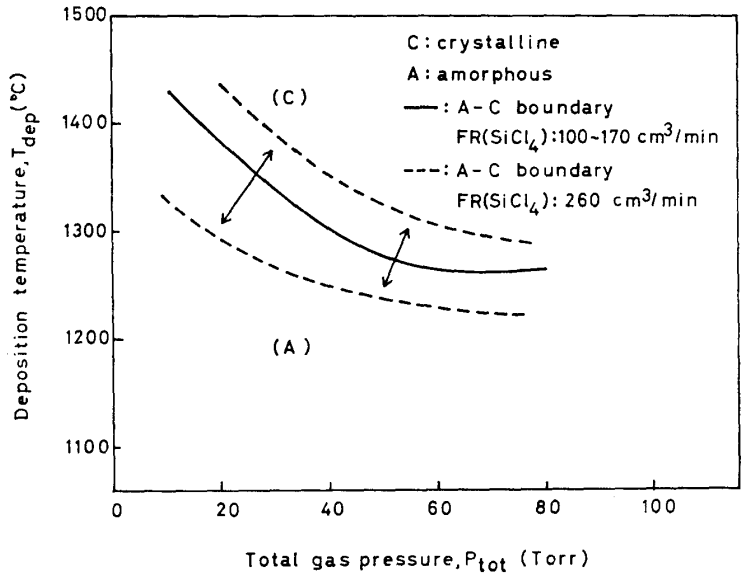

Fig. 2. Effect of deposition temperature (T_{dep}) and total gas pressure (P_{tot}) on the structure of CVD-Si_3N_4.

The silicon and oxygen contents of the CVD-amorphous Si_3N_4 determined by electron probe microanalysis are summarized in Table 2. The silicon contents of the amorphous deposits were close to the theoretical composition (60.08 wt%) as shown in Table 2. However, the oxygen content increased with decreasing T_{dep}.

The maximum thickness of the amorphous deposits obtained in the present experiments was 4.2 mm.

Table 2. Composition of the CVD-amorphous Si_3N_4 prepared at $FR(SiCl_4)=170$ cm³/min.

Preparation conditions		Composition (wt%)	
T_{dep} (°C)	P_{tot} (Torr)	Silicon	Oxygen
1200	40	59.1	2.2
1300	20	58.8	2.1
1400	10	58.8	1.6
Theoretical composition		60.08	0

III. 2 Structure and morphology

Figure 3 shows an electron micrograph and an electron diffraction pattern of the powdered sample deposited at $T_{dep}=1300$°C, $P_{tot}=10$ Torr and $FR(SiCl_4)=170$ cm³/min. Two diffused rings can be observed in Fig. 3b, indicating the amorphous structure of this sample. An X-ray diffraction profile also exhibits two broad lines, corresponding to the electron diffraction pattern (Fig. 3b).

Examples of the CVD-amorphous Si_3N_4 (with graphite substrate) are shown in Fig. 4. The thin amorphous deposits prepared under various conditions are translucent (Fig. 4a), while the thick ones show white color and metallic brightness (Fig. 4b).

Surface structures of the amorphous deposits prepared at $FR(SiCl_4)=170$ cm³/min can be divided into three types, as shown in Figs. 5~7. The first typical surface structure was formed at low T_{dep} below 1200°C and low P_{tot} below 20 Torr. As shown in Fig. 5 only the primary cone structure is observed in the deposits. Fig. 6 shows the second typical surface structure which was obtained at high T_{dep} and P_{tot}. In this case, each large primary cone is composed of small secondary cones. Fig. 7 indicates the third typical surface structure which was observed in the amorphous deposits formed under the A-C boundary condition. Large primary cones contain a large number of well-defined small secondary cones. The surface of secondary cones (Fig. 7b) is smooth and similar to that shown in Fig. 5.

Similar surface structures were observed in the amorphous deposits prepared at $FR(SiCl_4)=100$ and 260 cm³/min. Under these conditions, however, the deposits with the first typical surface structure (Fig. 5) were formed even at higher P_{tot} than that in the case of $FR(SiCl_4)=170$ cm³/min.

III. 3 Density

Figure 8 shows the relationship between density and P_{tot} for the CVD-amorphous Si_3N_4. The density of the deposits prepared at $T_{dep}=1100$ and 1200°C and at $FR(SiCl_4)=170$ cm³/min decreased with increasing P_{tot} in the range of 10 to 40 Torr, beyond which it increased with increasing P_{tot} in the range of 40 to 60 Torr and reached a constant value of about 2.76 g/cm³ above 60 Torr. The lowest and highest values of D were 2.76 g/cm³ (85% of the theoretical density of α-Si_3N_4, D_{th}: 3.18 g/cm³) and 2.86 g/cm³ (90% of D_{th}) at 1100°C, and 2.60 g/cm³(82%

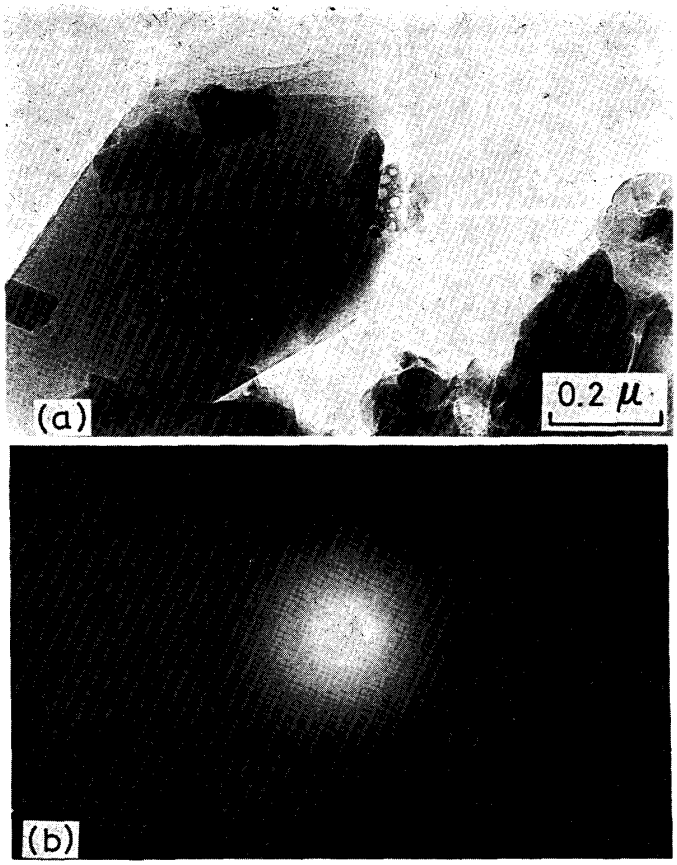

Fig. 3. Electron micrograph (a) and electron diffraction pattern (b) of the CVD-amorphous Si_3N_4 prepared at $T_{dep}=1300°C$, $P_{tot}=10$ Torr and $FR(SiCl_4)=170$ cm³/min.

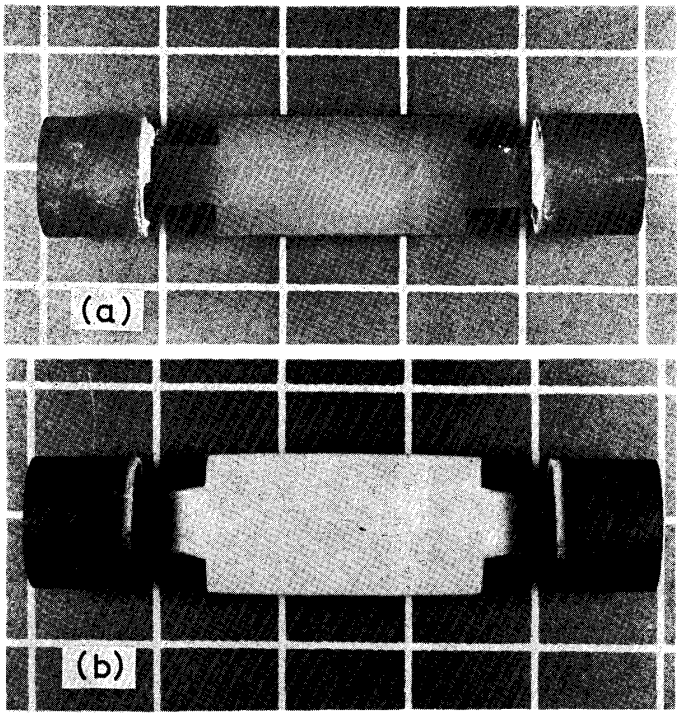

Fig. 4. The CVD-amorphous Si_3N_4 (1 div.=13 mm). (a) $T_{dep}=1100°C$, $P_{tot}=10$ Torr, FR $(SiCl_4)=170$ cm³/min, 2 hr; (b) $T_{dep}=1300°C$, $P_{tot}=30$ Torr, $FR(SiCl_4)=170$ cm³/min, 3 hr.

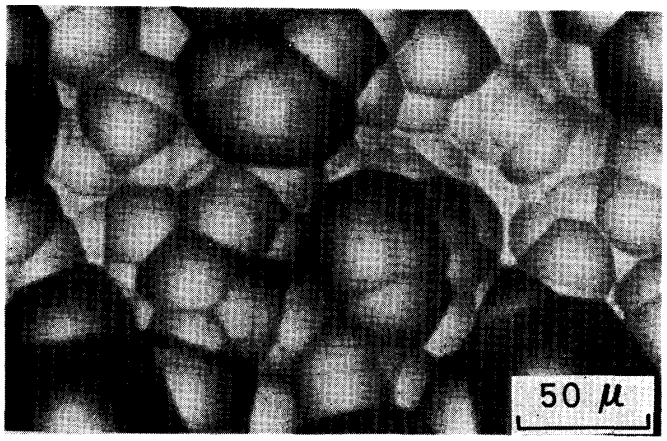

Fig. 5. Surface structure of the CVD-amorphous Si_3N_4 prepared at $T_{dep}=1200°C$, $P_{tot}=10$ Torr and $FR(SiCl_4)=170$ cm³/min.

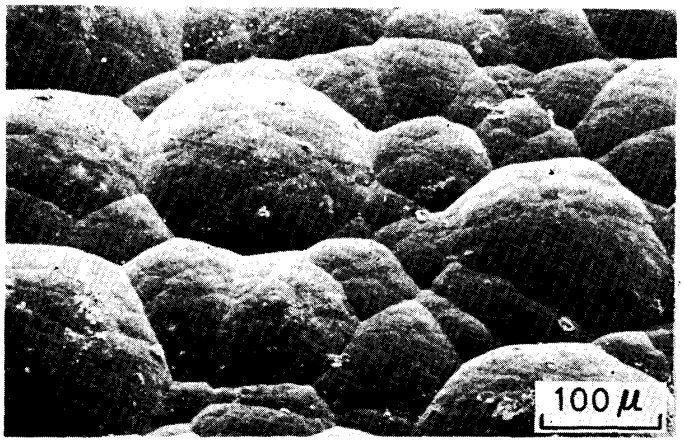

Fig. 6. Scanning electron micrograph of the surface of the CVD-amorphous Si_3N_4 prepared at $T_{dep}=1300°C$, $P_{tot}=30$ Torr and $FR(SiCl_4)=170$ cm³/min.

of D_{th}) and 2.83 g/cm³ (83% of D_{th}) at 1200°C, respectively.

However, the density of the amorphous deposits prepared at $T_{dep}=1200°C$ and $FR(SiCl_4)=100$ and 260 cm³/min was almost independent of P_{tot}. The highest value of D was 2.95 g/cm³ (92% of D_{th}) at $FR(SiCl_4)=100$ cm³/min and 3.00 g/cm³ (94% of D_{th}) at $FR(SiCl_4)=260$ cm³/min.

The density of the amorphous deposits prepared at $T_{dep}=1300$ and 1400°C and at $FR(SiCl_4)=170$ cm³/min was independent of P_{tot} and 2.88 and 2.89 g/cm³, respectively. At $T_{dep}=1200$ and 1300°C, the densities of the deposits obtained at $FR(SiCl_4)=100$ and 260 cm³/min are higher than that formed at $FR(SiCl_4)=170$ cm³/min.

III. 4 Deposition rate

Figure 9 shows the effect of P_{tot} on the rate of increase in thickness (x/t) of the CVD-amorphous Si_3N_4 at $T_{dep}=1100\sim1300°C$. As indicated in Fig. 9, the value of x/t increased with P_{tot}. At $T_{dep}=1100$ and 1200°C, the maximum value of x/t appeared at $P_{tot}=40\sim60$ Torr. The maximum x/t was 0.36 mm/hr under the condition of $P_{tot}=40$ Torr, $T_{dep}=1300°C$ and $FR(SiCl_4)=170$ cm³/min.

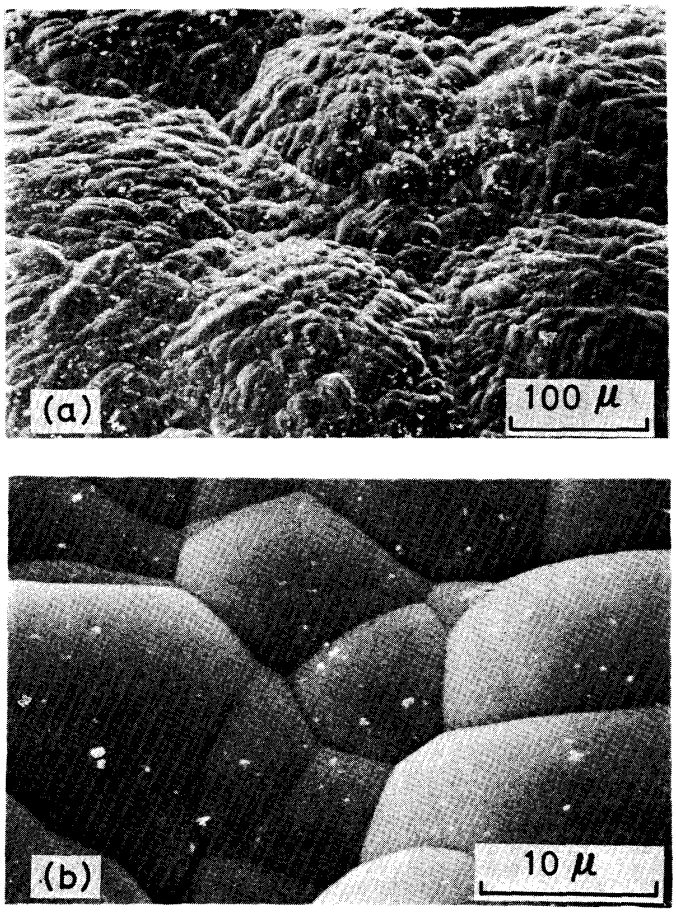

Fig. 7. (a) Scanning electron micrograph of the surface of the CVD-amorphous Si_3N_4 prepared at $T_{dep}=1400°C$, $P_{tot}=20$ Torr and $FR(SiCl_4)=170$ cm³/min; (b) scanning electron micrograph of (a) at higher magnification.

The time dependence of the thickness obeyed a linear law, where n is unity. Therefore, Eq. 3 leads to

$$k = Dx/t\,. \tag{4}$$

The relations between the deposition rate constant (k) as calculated from D and x/t data, and the reciprocal deposition temperature ($1/T_{dep}$) under various conditions are given in Fig. 10. The apparent activation energy (E) of formation of the CVD-amorphous Si_3N_4 was calculated from Fig. 10 to be 30 to 33 kcal/mol.

III. 5 Crystallization

To check the crystallization of the CVD-amorphous Si_3N_4, the amorphous deposits prepared under various conditions were heated at 1200~1500°C in Ar atmosphere for 6 hr or more and then examined by X-ray and electron diffraction techniques. The results are summarized in Table 3. In all cases, no crystallization occurred by heating at each T_{dep} for 6 hr. The amorphous deposits prepared at T_{dep} of 1100, 1200 and 1300°C were partly crystallized to α-Si_3N_4 by heating at temperature of 1300, 1300 and 1400°C, respectively.

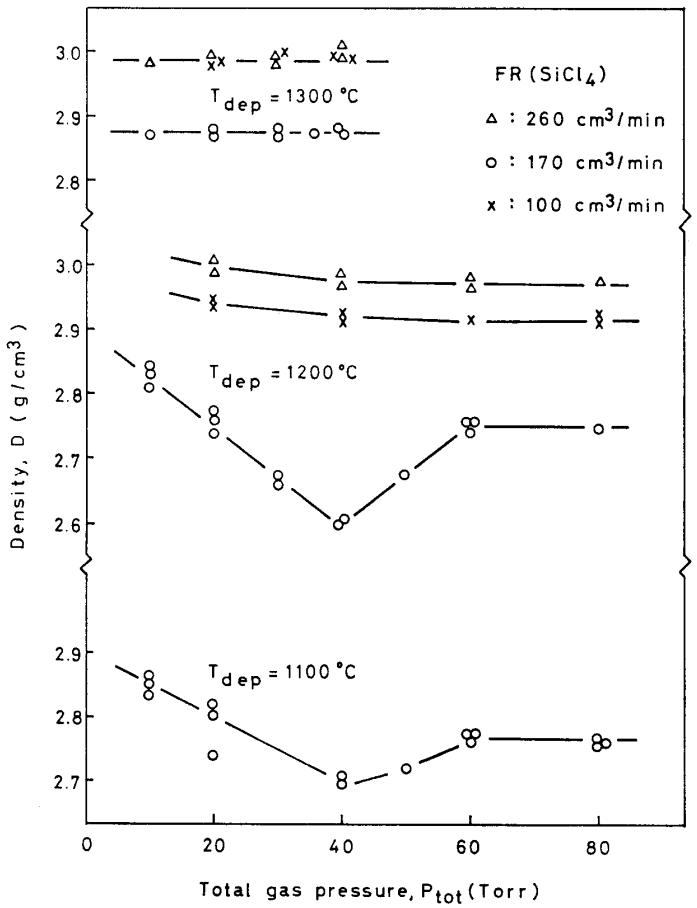

Fig. 8. Effect of total gas pressure (P_{tot}) on density (D) of the CVD-amorphous Si_3N_4.

III. 6 Thermal properties

The temperature dependence of the thermal constants of the CVD-amorphous Si_3N_4 at 20 to 1300°C was measured, and the values at 20 and 1300°C are listed in Table 4. The thermal diffusivity was 0.020 cm^2/sec at 20°C and decreased slightly with increasing temperature. The values of specific heat increased with increasing temperature. The thermal conductivity, calculated from the values of thermal diffusivity, specific heat and density, increased slightly from 0.010 cal/cm/sec/°C at 20°C to 0.012 cal/cm/sec/°C at 1300°C.

The thermal expansion coefficient from 20 to 1200°C, at which all the CVD-amorphous Si_3N_4 did not crystallize, was 2.99 ± 0.05/°C. The thermal expansion measurements were reversible. However, a small permanent contraction (~0.2 %) after cooling was observed when samples were heated up to a temperature higher than that for crystallization shown in Table 3.

III. 7 Hardness

Measurements of the Vickers microhardness at a 100-g load (VMH_{100}) of the CVD-amorphous Si_3N_4 prepared at FR($SiCl_4$)=170 cm^3/min were carried out for

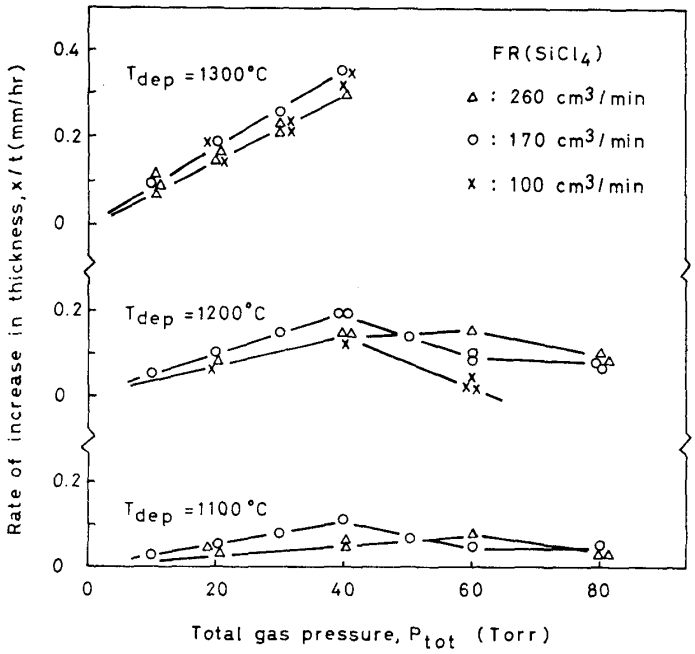

Fig. 9. Effect of total gas pressure (P_{tot}) on the rate of increase in thickness (x/t) of the CVD-amorphous Si_3N_4.

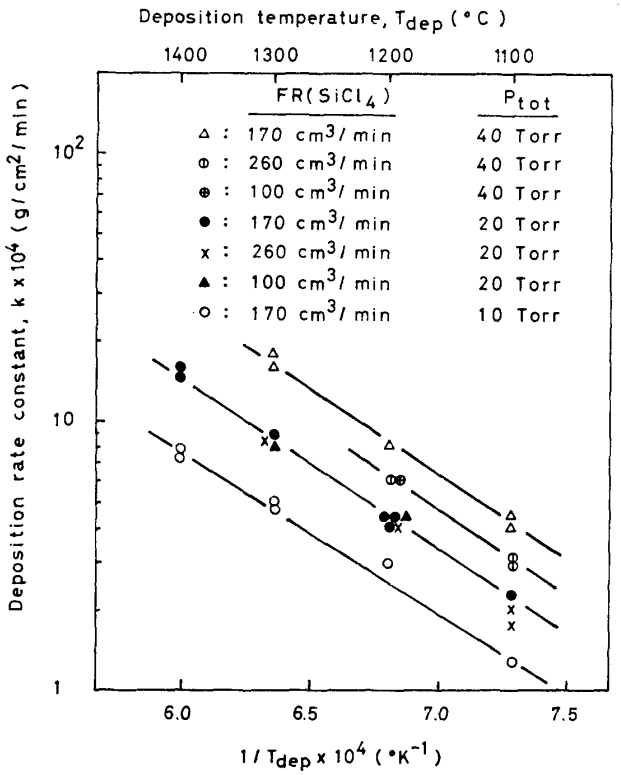

Fig. 10. Arrhenius plot of the deposition rate constant (k) of the CVD-amorphous Si_3N_4 under various deposition conditions.

Table 3. Crystallization of the CVD-amorphous Si_3N_4 prepared at $FR(SiCl_4)=170$ cm³/min.

Preparation conditions		HT*-temperature (°C)	HT*-time (hr)	Structural change
T_{dep} (°C)	P_{tot} (Torr)			
1100	40	1100	10	none
1100	40	1200	10	none
1100	40	1300	6	C**
1200	20	1200	10	none
1200	20	1300	6	C**
1300	30	1300	10	none
1300	30	1400	6	C**

HT*: heat treatment, C**: the crystalline α-Si_4N_3 was detected.

Table 4. Thermal constants of the CVD-amorphous Si_3N_4 with a density of 2.84 g/cm³ prepared at $T_{dep}=1300$°C, $P_{tot}=20$ Torr and $FR(SiCl_4)=170$ cm³/min.

Temperature (°C)	20	1300
Thermal diffusivity (cm²/sec)	0.020	0.013
Specific heat (cal/g/°C)	0.17	0.32
Thermal conductivity (cal/cm/sec/°C)	0.010	0.012

the deposition surface and the cross-section.

Figure 11 represents the relationship between VMH_{100} and P_{tot}. In this figure, only VMH_{100} on the deposition surface is plotted because the hardness values between the deposition surface and the cross-section were almost identical. The maximum and minimum VMH_{100} values were 3050 and 2200 kg/mm² at $T_{dep}=1100$°C, 3200 and 2700 kg/mm² at $T_{dep}=1200$°C and 3100 and 2300 kg/mm² at $T_{dep}=1300$°C, respectively.

The relation between VMH_{100} and T_{dep} is given in Fig. 12. VMH_{100} is particularly influenced by T_{dep} as indicated by curves a~e in the figure.

The Vickers hot-microhardness (VMH_{100}) of the CVD-amorphous Si_3N_4 from rt to 1300°C decreased slightly with increasing temperature and showed a value as high as 1200~1300 kg/mm² at 1300°C.

IV. Discussion

IV. 1 Density

Airey et al.[7] prepared the amorphous coatings of CVD-Si_3N_4 with $D=2.60\sim2.85$ g/cm³ at $T_{dep}=900\sim1100$°C using a SiH_4-NH_3 system, and those with $D=2.85\sim3.02$ g/cm³ at $T_{dep}=1150\sim1330$°C using a $SiCl_4$-NH_3 system. Chu et al.[6] obtained amorphous thin films with $D=2.78\sim3.10$ g/cm³ at $T_{dep}=850\sim1200$°C using SiH_4-NH_3 and $SiCl_4$-NH_3 systems. The relation between D and T_{dep} for the thin films, reported by Airey et al.[7] and Chu et al.[6], is shown in Fig. 13 and

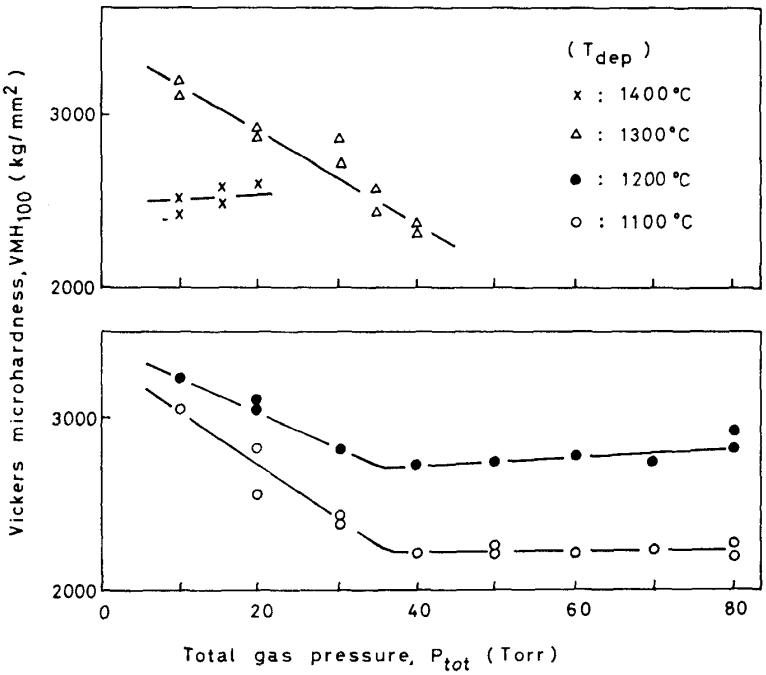

Fig. 11. Effect of total gas pressure (P_{tot}) on the Vickers microhardness (VMH_{100}) of the CVD-amorphous Si_3N_4 prepared at $FR(SiCl_4) = 170$ cm^3/min.

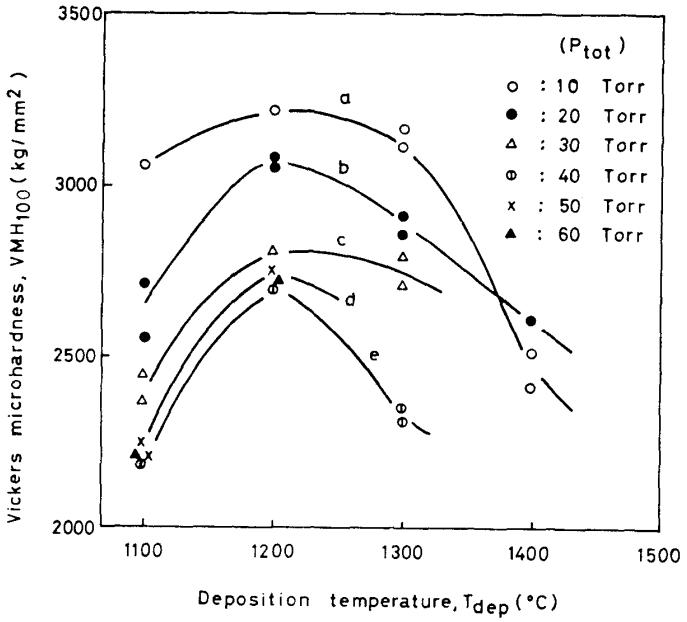

Fig. 12. Effect of deposition temperature (T_{dep}) on the Vickers microhardness (VMH_{100}) of the CVD-amorphous Si_3N_4 prepared at $FR(SiCl_4) = 170$ cm^3/min.

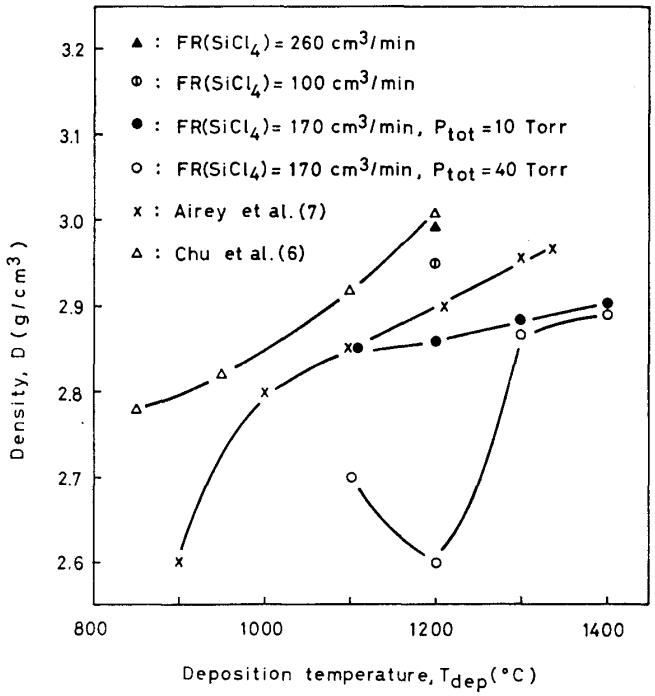

Fig. 13. The relation between deposition temperature (T_{dep}) and density (D) of the CVD-amorphous Si_3N_4.

compared with that observed for the massive CVD-amorphous Si_3N_4 in this work. The values of D for the massive amorphous deposits prepared at FR($SiCl_4$)=100 and 260 cm³/min are close to those of the thin films obtained by Chu et al.[6] However, the values of D for the massive amorphous deposits prepared at FR($SiCl_4$)=170 cm³/min depended markedly on P_{tot}. At low P_{tot} below 10 Torr, the values were close to those of Airey et al.,[7] but at P_{tot}=40 Torr a remarkable difference was observed.

For the massive amorphous deposits, D is closely related to the microstructure; the microstructure of the deposit with the lowest D value of 2.60 g/cm³ was composed of primary and secondary cones (Fig. 6), while the microstructure of the deposit with D=2.85 g/cm³ was composed solely of primary cones (Fig. 5). This behavior is quite similar to that observed in CVD-carbon.[14] At the cone boundaries the amorphous crystallites are irregularly aligned, so that the inter-crystallite porosities increase and consequently D decreases with increasing number of cone boundaries. The surface structures of the high-density massive amorphous deposits prepared at FR($SiCl_4$)=100 and 260 cm³/min mainly consisted of primary cones.

IV. 2 Structure

Chu et al.[6] reported that the CVD-amorphous Si_3N_4 films deposited at T_{dep}= 800~1000°C using the SiH_4-NH_3 and $SiCl_4$-NH_3 systems retained its amorphous

(14) T. Hirai and S. Yajima, J. Mater. Sci., **2** (1967), 18.

structure even after being annealed at 1200°C in N_2 atmosphere for 4 hr or longer.

As summarized in Table 3, in the present work the crystallization temperature of the massive CVD-amorphous Si_3N_4 deposits was remarkably affected by the deposition conditions such as T_{dep} and P_{tot}. This fact suggests that the structure of the amorphous deposits depends on the deposition conditions.

Bean et al.[5] measured the Knoop microhardness at a very low load of 8 g (KMH_8) and the Mohs' scale of hardness of the thin CVD-amorphous Si_3N_4 films of 1 μm thickness prepared using the SiH_4-NH_3 system. They reported KMH_8 was dependent upon the NH_3 concentration of the gas mixture. At 0.6% of NH_3, the CVD-amorphous Si_3N_4 exhibited a maximum hardness, KMH_8=3500 kg/mm^2, which can possibly be converted to VMH_{100}=2400 kg/mm^2 by using the empirical relationships between VMH and KMH and the load dependence of VMH.[15] They also reported that the Mohs' hardness increased with increasing T_{dep} up to T_{dep}= 900°C, but independent of T_{dep} at T_{dep}=900$\sim$1200°C.

In the present study, the VMH_{100} value of the massive CVD-amorphous Si_3N_4 was strongly affected by the deposition conditions, especially T_{dep} and P_{tot}, and varied between 2200 and 3200 kg/mm^2. These hardness values are much higher than the VMH_{50} value of 1260 kg/mm^2 reported for the fused silica.[16] As shown in Fig. 14, the relation between VMH_{100} and density shows a different behavior at each T_{dep}. This implies the difference in structure of the CVD-amorphous Si_3N_4 prepared at different T_{dep}.

It is well known that the thermal conductivity is related to the specific heat and the velocity and mean free path of phonon. The mean free path of phonon in the CVD-amorphous Si_3N_4 was estimated to be about 10 Å taking 5×10^5 cm/sec as a representative value of the phonon velocity.[17] The value of about 10 Å may correspond to the size of the cluster in the CVD-amorphous Si_3N_4.

Coleman et al.[18] prepared the amorphous SiO_2 films by a glow discharge CVD of a N_2O-SiH_4 mixture. This deposit consisted of a mixture of silicon and silica. From the radial distribution function (RDF), the silicon and silica particles were estimated to have a minimum diameter of approximately 10 Å and a maximum size of not more than about 20 Å. They also prepared thin CVD-amorphous Si_3N_4 films at T_{dep}=300°C using a NH_3-SiH_4 mixture by a glow discharge method. On the basis of the measured RDF, they proposed that the minimum diameter of the clusters in the CVD-amorphous Si_3N_4 films was about 8$\sim$10 Å.

The size of the clusters of the CVD-amorphous Si_3N_4 calculated from the thermal constants in the present work is in good agreement with those of Coleman et al.[18] for amorphous silicon, silica and Si_3N_4.

(15) K. Niihara and T. Hirai, J. Mater. Sci., in press.
(16) W.G. Bradshaw and C.O. Mathews, *Properties of Refractory Materials; Collected Data and References*, LMSD-2466 (June 24, 1958).
(17) C. Kittel, *Introduction to Solid State Physics*, John Wiley, New York, (1971), p. 225.
(18) M.V. Coleman and D.J.D. Thomas, Phys. Stat. Sol., **25** (1968), 25.

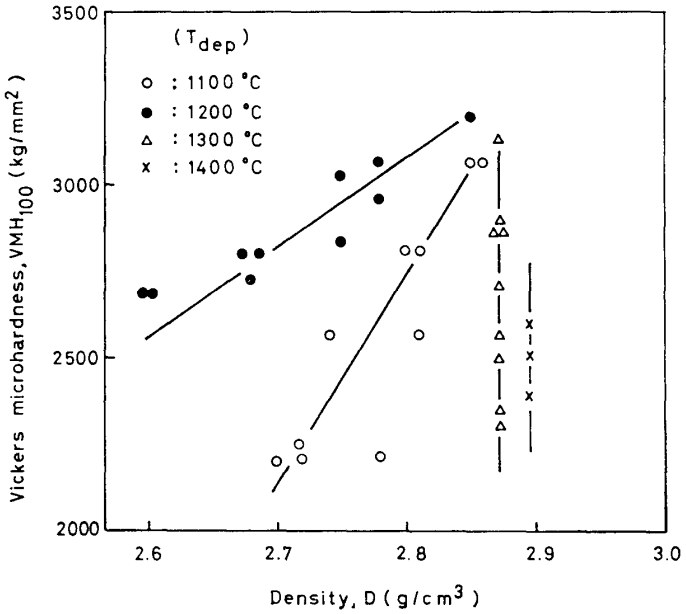

Fig. 14. Effect of density of the Vickers microhardness (VMH_{100}) of the CVD-amorphous Si_3N_4 prepared at $FR(SiCl_4)=170$ cm³/min.

The structure in a short range order within the minimum particle size of about 10 Å seems to be not appreciably affected by T_{dep} and P_{tot}. Thus, the structural variation in the CVD-amorphous Si_3N_4 with T_{dep} and P_{tot} seems to be attributed to the structural characteristic among the particles. For the CVD-carbon, it is known that there are cross-links among the crystallites and the characteristics of the cross-links are affected by the deposition conditions.[14]

IV. 3 Deposition rate

A plot of deposition rate as a function of P_{tot} in Fig. 9 indicates maxima in x/t at $P_{tot}=40\sim60$ Torr. The present experiments were carried out at constant mass flow rates. Decrease in the deposition rate at higher P_{tot} may be due to the homogeneous reactions which lead to powder formation. These homogeneous reactions depend on the time during which intermediates stay in the hot zone surrounding the substrate and on the occurrence of free convection in the gas phase.

Sparrow et al.[19] derived the ratio Gr/Re^2, i.e., the ratio of buoyancy forces to inertial forces, in order to evaluate the gas flow over a hot surface:

$$Gr/Re^2 = \frac{gH(T_1-T_0)}{4T_0v^2}, \tag{5}$$

where Gr is the Grashof number, Re the Reynolds number, g the gravity, H the distance between the substrate and the reactor wall, T_1 the substrate temperature, T_0 the wall temperature, and v the gas velocity. The ratio Gr/Re^2 increases with

(19) E.M. Sparrow, R. Eichhorn and J.L. Gregg, Phys. Fluids, **2** (1959), 319.

increasing P_{tot}. For the pure forced convection, the value should be less than 0.3. Furthermore, in the present experiments the buoyancy force has a component in the direction opposite to the flow of gases. The flow separation occurs in the case of $Gr/Re^2>1$ and then the gas flow is upward near the deposition surface.

In the present work, Gr/Re^2 is calculated to be $0.3\sim0.4$ at $P_{tot}=40$ Torr and FR ($SiCl_4$)=100 and 170 cm^3/min, and about 0.35 at $P_{tot}=60$ Torr and FR($SiCl_4$)= 260 cm^3/min. Consequently, the forced convection occurs below about 40 Torr at FR($SiCl_4$)=100 and 170 cm^3/min and below about 60 Torr at FR ($SiCl_4$)=260 cm^3/min.

It is apparent from the numerical considerations on the gas flow pattern that the deposition rate increases with P_{tot} up to the P_{tot} at which the overall flow varies from the forced convection (downward) to the free convection (upward).

The apparent activation energy for the CVD-amorphous Si_3N_4 formation is $30\sim33$ kcal/mol, independent of P_{tot} and FR. The formation of the CVD-amorphous Si_3N_4 involves complex processes such as decomposition and reaction of reactants, polymerization of intermediates and growth of nuclei in the gas phase or on the deposition surface. On the other hand, $SiCl_4$ reacts with NH_3 even at room temperature.[20-22]

$$SiCl_4+6\ NH_3 \rightarrow Si(NH)_2+4\ NH_4Cl \tag{6}$$

$Si(NH)_2$ readily polymerizes with increasing temperature, and its pyrolysis yields α-Si_3N_4 according to the following reactions:

$$6[Si(NH)_2]_n \xrightarrow[-2NH_3]{400^\circ C} 2[Si_3(NH)_3N_2]_n$$

$$\xrightarrow[-NH_3]{650^\circ C} 3[Si_2(NH)N_2]_n \xrightarrow[-2NH_3]{1200^\circ C} 2\alpha\text{-}Si_3N_4\,. \tag{7}$$

As seen in reactions 6 and 7, various intermediates contribute to Si_3N_4 formation. Unfortunately, there are almost no thermochemical data concerning various complex intermediates in the $SiCl_4$-NH_3 system. Therefore, it is difficult to define the implication of the E value and hence the formation mechanism of the massive CVD-amorphous Si_3N_4.

V. Conclusion

(1) Massive CVD-amorphous Si_3N_4 up to 4.2 mm thick was successfully prepared. The preparation of the CVD-amorphous Si_3N_4 depended markedly on T_{dep}, P_{tot} and FR($SiCl_4$).

(2) The silicon contents of the amorphous deposits were close to the theoretical

(20) M. Billy, Ann. Chem., **4** (1959), 795.
(21) O. Glemser and P. Naumann, Z. Anorg. Allgem. Chem., **298** (1958), 134.
(22) K.S. Mazdiyasni and C.M. Cooke, J. Amer. Ceram. Soc., **56** (1973), 628.

composition, although 1.6～2.0 wt% of oxygen is contained in the deposits.

(3) For the CVD-amorphous Si_3N_4, three types of cone structure were observed; (a) primary cones at low T_{dep} and P_{tot}, (b) large primary cones composed of secondary cones at high T_{dep} and P_{tot}, and (c) large primary cones composed of a large number of well-defined secondary cones at the A-C boundary.

(4) The density of the CVD-amorphous Si_3N_4 prepared at FR($SiCl_4$)=170 cm^3/min depended strongly on T_{dep} and P_{tot}, while the density at FR($SiCl_4$)=100 and 260 cm^3/min was almost independent of P_{tot}. The lowest and highest densities were 2.60 g/cm^3 at T_{dep}=1200°C, P_{tot}=40 Torr and FR($SiCl_4$)=170 cm^3/min and 3.00 g/cm^3 at T_{dep}=1200°C, P_{tot}=20 Torr and FR($SiCl_4$)=260 cm^3/min, respectively.

(5) At T_{dep}=1100 and 1200°C, a maximum value of the deposition rate (x/t) of the CVD-amorphous Si_3N_4 appeared at P_{tot}=40～60 Torr. The maximum x/t was 0.36 mm/hr at P_{tot}=40 Torr, T_{dep}=1300°C and FR($SiCl_4$)=170 cm^3/min.

(6) The activation energy of the CVD-amorphous Si_3N_4 formation was 30～33 kcal/mol, independent of P_{tot} and FR.

(7) The CVD-amorphous Si_3N_4 prepared at T_{dep} of 1100～1300°C did not crystallize by heat treatment at each T_{dep}.

(8) The thermal conductivity of the CVD-amorphous Si_3N_4 increased slightly from 0.010 cal/cm/sec/°C at 20°C to 0.012 cal/cm/sec/°C at 1300°C.

(9) The thermal expansion coefficient of the CVD-amorphous Si_3N_4 from 20 to 1200°C was 2.99±0.05/°C.

(10) The Vickers microhardness (VMH_{100}) of the CVD-amorphous Si_3N_4 was dependent on T_{dep} and P_{tot}, and the maximum and minimum VMH_{100} values were 3200 kg/mm^2 at T_{dep}=1100°C and 2200 kg/mm^2 at T_{dep}=1200°C, respectively.

(11) The hot hardness VMH_{100} was 1200～1300 kg/mm^2 at 1300°C.

Acknowledgements

The authors would like to express their appreciation to Messrs. T. Kinoshita and M. Sobajima of Nippon Kogaku, Ltd. for carring out the Vickers hot-microhardness measurements. This research was supported in part by the scientific research fund from the Ministry of Education, Contract No. 047015.